Biophysical Chemistry 193–194 (2014) 1–8

Contents lists available at ScienceDirect

Biophysical Chemistry

journal homepage: http://www.elsevier.com/locate/biophyschem

Characterization of the non-specific DNA binding properties of the Adenoviral IVa2 protein ☆

Teng-Chieh Yang [a], Nasib Karl Maluf [a,b,*]

[a] University of Colorado Denver, School of Pharmacy, Dept. Pharm. Sciences, C238 12850 E. Montview Blvd., V20-4121, Aurora, CO 80045
[b] Alliance Protein Laboratories, 6042 Cornerstone Ct West A, San Diego, CA 92121

HIGHLIGHTS

- Non-specific DNA binding of the adenoviral IVa2 protein was characterized.
- Novel quantitative approach allowed rigorous characterization of DNA binding.
- IVa2 binds non-specific DNA with strong nearest neighbor cooperativity.
- Proposed IVa2 recruits other viral proteins to initiate virus assembly.

GRAPHICAL ABSTRACT

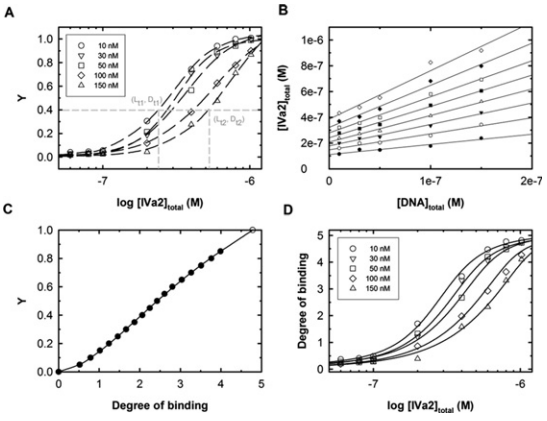

ARTICLE INFO

Article history:
Received 6 June 2014
Received in revised form 19 June 2014
Accepted 19 June 2014
Available online 28 June 2014

Keywords:
IVa2
Virus assembly
McGhee and von Hippel non-specific binding model
Non-specific DNA binding
Analytical ultracentrifugation
Sedimentation equilibrium

ABSTRACT

Human Adenovirus (Ad) is a non-enveloped, icosahedral virus with a linear, double-stranded DNA genome. The Ad IVa2 protein is involved in multiple viral processes including viral late gene transcription and virus assembly. Previous studies have shown that IVa2 loads additional viral proteins onto conserved DNA elements within the Ad genome to regulate these viral processes. IVa2 also possesses strong non-specific DNA binding activity, and it is likely it uses this activity to recruit proteins to the conserved DNA elements. Here we have investigated the non-specific DNA binding activity of IVa2 using nitrocellulose/DEAE filter binding and sedimentation equilibrium techniques. We have analyzed our data using the McGhee and Von Hippel approach [1], and find that IVa2 binds with strong, positive nearest-neighbor cooperativity. In addition, we describe how to apply the McGhee and von Hippel approach to directly analyze sedimentation equilibrium data using non-linear least-squares methods. We discuss the implications of these results with respect to current virus assembly mechanisms.

Abbreviations: Ad, adenovirus; MLP, major late promoter; PS, packaging sequence; EMSA, electrophoresis mobility shift assay; NC, nitrocellulose; MvH, McGhee and von Hippel; NLLS, non-linear least square; MBDF, macromolecular binding density function.

☆ Funding: This work was supported by start-up funds provided by the Department of Pharmaceutical Sciences, School of Pharmacy, University of Colorado Denver.

* Corresponding author at: Alliance Protein Laboratories, 6042 Cornerstone Ct West A, San Diego, CA 92121. Tel.: +1 858 550 9401; fax: +1 858 550 9403.
E-mail address: Karl.Maluf@ap-lab.com (N.K. Maluf).

http://dx.doi.org/10.1016/j.bpc.2014.06.005
0301-4622/

1. Introduction

Human adenovirus (Ad) is a non-enveloped, icosahedral virus with a linear double stranded DNA genome. Ad infection has been found in several organs and tissues [2,3], and is potentially lethal in immunocompromised patients [4,5].

The Ad IVa2 protein is a multifunctional regulator of the Ad lifecycle. IVa2 is involved in several viral processes including viral late gene transcription and virus assembly/genome packaging. IVa2 was first identified as a transcriptional activator of the viral major late promoter (MLP) which predominantly controls the genes encoding viral structural proteins [6–8]. Additional *in vivo* and *in vitro* studies have shown that the genome packaging process requires at least three viral components: the IVa2 and L4-22 K proteins, and a conserved region within the Ad genome, called packaging sequence (PS) [9–13]. The PS DNA (~200 bp) is composed of multiple recognition elements, called A repeats, which contain the following consensus sequence: 5'-TTTG (N_8) CGXG-3'. The wild type PS DNA contains 4 exact copies of this consensus sequence, called AI, AII, AV, AVI. Additional "half sites," which contain either TTTG or CGXG motifs, are also present. While deletion of the wild type PS DNA is lethal for virus assembly, there are several additional arrangements of A repeats that can support the viral lifecycle. In particular, replacing the PS DNA with two adjacent copies of the A-I-II sequence (i.e. I-II-I-II) rescues wild type viral replication activity [14].

Electrophoresis Mobility Shift Assay (EMSA) studies using Ad-infected nuclear extracts, along with a probe encompassing the A-I-II repeats, showed that the IVa2 and L4-22 K proteins specifically interact with A repeat DNA such that IVa2 recognizes the CGXG motif and L4-22 K *requires* IVa2 to interact with the TTTG motif [9,11,13–15]. Our previous studies, using the same A-I-II DNA, suggest IVa2 binds to the CGXG motif with *apparent* low specificity (~10 fold stronger affinity binding to A-I-II DNA than to a non-specific DNA of *identical length*) [16]. Thus, true specificity requires the presence of both L4-22 K and IVa2 proteins interacting with the consensus 5'-TTTG (N_8) CGXG-3' sequences [17]. While the L4-22 K protein does not bind DNA (i.e. DNA with or without the TTTG sequence) by itself, the IVa2 protein does [17]. Therefore, a tempting hypothesis is that IVa2's non-specific DNA binding activity is required to recruit L4-22 K to the A sequences.

To develop a complete quantitative understanding of how the IVa2 and L4-22 K proteins together specifically recognize the A repeats and therefore regulate the viral lifecycle, we first need to determine the non-specific binding properties of the IVa2 protein. We report here a novel application of nitrocellulose/DEAE filter binding, along with analytical ultracentrifugation, to quantify fundamental thermodynamic parameters such as the non-specific DNA binding site size, affinity and nearest neighbor cooperativity. We discuss these results in the context of current virus assembly hypotheses.

2. Materials and methods

2.1. IVa2 protein and buffer preparation

The IVa2 protein used in this and all our previous studies is an N-terminal truncated protein starting at amino acid Met 75, which has been shown previously to possess wild type viral activity [18]. This protein was overexpressed in *E. coli.* BL21 (DE3) and purified to homogeneity as described previously [16], and its DNA binding activity was determined as described previously [16]. All experiments were carried out in Buffer H (100 mM NaCl, 40 mM HEPES, pH 7.6 at 25 °C, 10 % (v/v) glycerol, 5 mM 2-mercapato ethanol and 1 mM EDTA).

2.2. DNA preparation

For the preparation of the 109 bp DNA, the pUC19 vector (Invitrogen) was transformed into *E. coli.* DH5 alpha, grown overnight in 1 L LB (37 °C), and purified using QIAGEN Plasmid Maxi kits. The 109 bp DNA was excised from purified pUC19 using BspHI and separated by gel electrophoresis. The final 109 bp DNA has > 99.9% purity as judged by densitometry analysis as well as ^{32}P-labeleing using the Klenow fill-in reaction. The concentration of purified 109 bp DNA was determined by UV spectroscopy using the calculated extinction coefficient of 1.357 μM^{-1} cm^{-1}.

For the preparation of the 241 bp DNA, we constructed a vector (pQY103) containing Ad genomic DNA from position 91 to 300 using pUC19. The DNA was amplified by PCR technique using Ad virus genomic DNA as the template. The primer sequences were as follows: forward: 5'-CCGGATCCGCGGGTGACGTAGTAGTGTGG-3'; reverse: 5'-TCCTGTCGACTCCTCTTATTCAGTTTTCCCGCG-3'. The BamHI and SalI restriction sequence are underlined. The amplified DNA was cleaved by BamHI and SalI, then cloned into pUC19. The sequence fidelity was confirmed by DNA sequencing. The pQY103 was purified as described above and digested with SmaI and HindIII. The purified DNA was labeled and its concentration determined using the calculated extinction coefficient of 3.001 μM^{-1} cm^{-1} at 260 nm.

The 241 bp (Cy3) DNA was prepared using preparative PCR. The pQY103 vector was amplified using Cy3 labeled primers:

forward: 5'Cy3-GGGGATCCGCGGGTGACGTAGTAG-3'

reverse: 5' Cy3-AGCTTGCATGCCTGCAGGTCGAC-3'

The amplified PCR reaction (1 mL) was batch-loaded onto a Q FF resin (500 μL bead volume equilibrated with TE buffer — 10 mM Tris and 1 mM EDTA at pH 8.0, with 500 mM NaCl) (GE). The column was flushed with 1.5 mL of TE buffer with 600 mM NaCl to wash off the unincorporated primers. The 241 bp (Cy3) DNA was eluted with TE buffer plus 700 mM NaCl and then precipitated by ethanol. The DNA was > 99.9% pure as judged by densitometry analysis. The concentration of purified 241 bp (Cy3) DNA was determined by UV spectroscopy using a calculated extinction coefficient of 3.001 μM^{-1} cm^{-1} at 260 nm. The percentage of 241 bp (Cy3) DNA with end-labeled Cy3 dyes was calculated using the extinction coefficient of 0.0869 μM^{-1} cm^{-1} for a single Cy3 dye at 522 nm [16] and the ratio of the absorbance at 522 to 260 nm (A_{522}/A_{260}). For each preparation of the 241 bp (Cy3) DNA, the A_{522}/A_{260} is between 0.046 and 0.049, which returns the average 80%–85% of the 241 bp (Cy3) DNA has end-labeled Cy3 dyes.

2.3. Double membrane filter binding titrations

Filter binding titrations were carried out as described by Wong et al. [19] with the following modifications. Three nitrocellulose (NC) membranes (Hybond-ECL from GE) were layered on top of three DE81 membranes (Whatman). The nitrocellulose membranes will bind protein and protein-DNA complexes, but not the unbound DNA. The DE81 membranes bind the free DNA. Both membranes were incubated in Buffer H for at least 30 min then inserted into a Minifold I Dot-Blot System (96 wells, Schleicher & Schuell). For our system, we found that a single nitrocellulose and DE81 membrane pair was unable to retain all the ^{32}P-labeled materials. Each reaction contained 1200 cpm of ^{32}P-labeled DNA, and when appropriate, non-labeled DNA was added to the indicated final concentration. All reactions were carried out in Buffer H, and were equilibrated at 25 °C for at least 50 min prior to filtration. 150 μL of Buffer H was passed through each well, followed by 25 μL of each reaction mixture, and finally each well was washed with an additional 150 μL of Buffer H. The membranes were exposed overnight to a phosphoimager screen (GE) and the intensity of each spot was quantified by densitometry analysis using Imagequant (GE). The fraction of the signal retained on the NC membranes was calculated using $Y = S_{NC}/(S_{DE} + S_{NC})$, where S_{NC} and S_{DE} are the total intensity from the three NC and DE membranes for each spot. To test whether the experiments reached equilibrium, we doubled the incubation time to 100 min; we saw no difference in the resulting isotherms.

2.4. Analysis of filter binding titrations

The filter binding method provides quantitative information on the fraction of DNA molecules bound as a function of ligand (protein) concentration. When these experiments are performed as a function of DNA concentration, information on the extent of binding of the protein ligand to the DNA molecule (moles of ligand bound per mole of DNA) can be obtained in a model independent manner [20,21]. We describe the application of this approach to our filter binding data in detail in the results section. The resulting binding isotherms (expressed as moles of bound ligand per mole of linear DNA molecule) were analyzed by the approach of McGhee and von Hippel (MvH) in order to quantify the non-specific DNA binding properties of the IVa2 protein [1,22,23] using Eqs. (1) and (2):

$$\nu = K_{ns} \cdot L_f \cdot (1-n\nu) \cdot (ff)^{(n-1)} \cdot \left(\frac{1-(n+1)\nu+R}{2(1-n\nu)}\right)^2 \cdot \left(\frac{S-n+1}{S}\right) \quad (1)$$

where $(ff) = \frac{2w\cdot(1-n\nu)}{(2w-1)\cdot(1-n\nu)+\nu+R}$ and

$$R = \sqrt{[1-(n+1)\cdot\nu]^2 + 4w\nu\cdot(1-n\nu)} \quad (2)$$

$$\overline{X} = S\cdot\nu.$$

where K_{ns} is the intrinsic non-specific binding constant, L_f is the concentration of free ligand, n is the non-specific occluded site size (in bp), S is the length of the DNA molecule (in bp unit), w is the nearest-neighbor cooperativity, ν is the binding density, i.e. the number of ligands bound per bp, $\overline{X}$ is the degree of binding, i.e. the average number of ligand bound per linear DNA molecule [24], and (ff) denotes the conditional probability of finding one free bp adjacent to a free bp [1]. The term $(S - n + 1)/S$ in Eq. (1) has been shown to adequately approximate end effects for relatively short DNA molecules [23]. According to mass conservation,

$$L_t = L_f + L_b = L_f + S\cdot\nu\cdot D_t \quad (3)$$

where L_b is the concentration of bound ligand and D_t is the total DNA concentration in linear DNA molecule units. Combining Eqs. (1) and (3) yields the expression for total ligand concentration:

$$L_t = \frac{\nu}{K_{ns}\cdot(1-n\nu)\cdot(ff)^{(n-1)}\cdot\left(\frac{1-(n+1)\cdot\nu+R}{2(1-n\nu)}\right)^2\cdot\left(\frac{S-n+1}{S}\right)} + S\cdot\nu\cdot D_t \quad (4)$$

During the data-fitting procedure, one implicitly solves Eq. (4) for ν for a given L_t and D_t. This model was used to globally analyze the set of binding isotherms as a function of both protein and DNA concentrations.

2.5. Sedimentation equilibrium experiments

Analytical ultracentrifugation experiments were performed using a Beckman XLA centrifuge equipped with an eight-hole rotor and a monochromator set to 522 nm. Sedimentation equilibrium experiments were carried out in Buffer H at 25 °C using 6 sector centerpieces, where 115 μL of sample and 120 μL of reference buffer were loaded into their respective chambers. The experiments were performed at the indicated speeds and the data were collected using a radial step size of 0.001 cm with 20 replicates in the step mode. All experiments were judged to have reached equilibrium using the Winmatch program [25]. To estimate the z-average molecular weight [26] of each loading ratio of IVa2:DNA, the data were initially analyzed using a model which includes a single, ideal sedimenting species using the program Winnonlin, according to the following equation:

$$A_{t,r} = A_{t,\mathrm{ref}}\cdot\exp\left(\frac{M_{b,app}\cdot\omega^2}{RT}\cdot\frac{r^2-r_{ref}^2}{2}\right) + b \quad (5)$$

where $A_{t,r}$ is the total absorbance at radial position r, $A_{t,ref}$ is the total absorbance at the reference radial position r_{ref}, ω is the angular velocity of the rotor, R is the gas constant, T is the absolute temperature, b is the baseline offset and $M_{b,app}$ is the apparent buoyant molecular weight, given by:

$$M_{b,app} = M_{app}\cdot\left(1-\overline{\upsilon}_{app}\rho\right) \quad (6)$$

where M_{app} is the apparent molecular weight of the species and $\overline{\upsilon}_{app}$ is the apparent partial specific volume of the species, and ρ is the buffer density. The fitted $M_{b,app}$ is used to calculate the approximate average number of IVa2, m, bound to a single DNA molecule according to Eq. (7)

$$M_{b,app} = M_{b,DNA} + m\cdot M_{b,IVa2} \quad (7)$$

where $M_{b,IVa2}$ is 10.1(±0.7) kDa. We also used sedimentation equilibrium to determine the $M_{b,DNA}$ of the 241 bp DNA to be 63.1(±1.3) kDa which returns a partial specific volume of 0.561(±0.01) cm^3/g.

2.6. NLLS analysis of sedimentation equilibrium data using the McGhee–von Hippel non-specific binding model

The following derivation assumes there is no significant volume change associated with the protein-DNA binding reaction. In order to use the MvH non-specific binding model for NLLS analysis of our sedimentation equilibrium data, we substituted the expression for an ideally sedimenting free ligand (i.e. the IVa2 monomer) into Eq. (1), which yields Eq. (8):

$$\nu = K_{ns}\cdot\left[L_{f,m}\cdot\exp\left(\frac{M_L(1-\overline{\upsilon}_L\rho)\cdot\omega^2}{RT}\cdot\frac{r^2-r_m^2}{2}\right)\right]\cdot(1-n\nu) \cdot(ff)^{(n-1)}\cdot\left(\frac{1-(n+1)\nu+R}{2(1-n\nu)}\right)^2\cdot\left(\frac{S-n+1}{S}\right) \quad (8)$$

where $L_{f,m}$ denotes the concentration of free ligand (IVa2) at meniscus position, r_m, M_L is the molecular weight of free ligand (Da), and $\overline{\upsilon}_L$ is the partial specific volume of free ligand. The binding density ν, which is a function of the radial position, is calculated implicitly at each radial position using the Scientist software (Micromath, St. Louis MO).

We calculated the concentration of free DNA from the conditional probability of having $(S - 1)$ consecutive free bp next to the first free bp [23] according to:

$$D_f = D_t\cdot(1-n\nu)\cdot(ff)^{S-1} \quad (9)$$

To obtain an expression for the total DNA as a function of the radial position, we substituted the expression for an ideal sedimenting DNA species into Eq. (9), which yielded:

$$D_{t,r} = \frac{D_{f,m}\cdot\exp\left(\frac{M_D\cdot(1-\overline{\upsilon}_D\rho)\cdot\omega^2}{RT}\cdot\frac{r^2-r_m^2}{2}\right)}{(1-n\nu)\cdot(ff)^{S-1}} \quad (10)$$

where $D_{f,m}$ denotes the concentration of free (i.e. unbound) DNA at the reference radial position (taken as the meniscus position), M_D is the molecular weight of the free DNA (Da), and $\overline{\upsilon}_D$ is the partial specific volume of the free DNA. Combining Eqs. (10) and (11), we directly analyzed, by NLLS, the absorbance data according to Eq. (12), using 1.2 cm for the path length l. The ε_{522nm} for 241 bp DNA was determined to be 0.18 $\mu M^{-1}\,cm^{-1}$.

$$Abs_r = D_{t,r}\cdot\varepsilon_{522nm}\cdot l \quad (11)$$

$$Abs_r = \frac{D_{f,m} \cdot \exp\left(\frac{M_D \cdot (1-\overline{v}_D\rho) \cdot \omega^2}{RT} \cdot \frac{r^2 - r_m^2}{2}\right)}{(1-n\nu) \cdot (ff)^{S-1}} \cdot \varepsilon_{522nm} \cdot l + b \qquad (12)$$

During the data-fitting procedure, Eq. (12) is solved at each radial position using the corresponding ν calculated from Eq. (8). This approach allows us to treat the binding site size, n, as a continuous fitting parameter, in contrast to other approaches [25].

Mass conservation approach for sedimentation equilibrium analysis

According to mass conservation in a rectangular cell, the initial loading concentration of the ligand, L_0, and the macromolecule, D_0, are given by Eqs. (13) and (14) [16,27]:

$$L_0 = \frac{1}{(r_b - r_m)} \int_{r_m}^{r_b} L_{T,r}\, dr \qquad (13)$$

$$D_0 = \frac{1}{(r_b - r_m)} \int_{r_m}^{r_b} D_{T,r}\, dr \qquad (14)$$

where r_b is the bottom position of the solution column (i.e. the base of the cell), and r_m is the radial position of the sample meniscus. r_m is taken as the peak of the meniscus artifact, and r_b was estimated using Eq. (13) along with the known DNA loading concentration.

3. Results

To characterize the thermodynamics of non-specific binding of IVa2 to dsDNA, we used the double membrane filter binding approach discussed by Wong and Lohman [19]. These experiments were performed by titrating a nonspecific 109 bp DNA with the IVa2 protein in Buffer H (25 °C). The experiments were carried out at 5 constant concentrations of DNA. We quantified the radioactivity retained on both the NC and DE81 membranes in order to calculate the fraction of the total added DNA retained on the NC membrane (Fig. 1A). Most of the isotherms reach plateaus within one order of magnitude of the total IVa2 concentration, which implies strong positive cooperativity for IVa2-DNA binding. As previously discussed, different protein-DNA ligation states might exhibit different filter retention efficiencies, and consequently, there is no a priori reason to assume a linear relationship between filter retention efficiency and degree of binding [19,28]. To account for this, we used the model-independent macromolecular binding density function (MBDF) approach [20,21] to directly convert the filter retention signal into the degree of binding. The details of this analysis are discussed below.

To facilitate the interpolation required in the MBDF analysis, each isotherm in Fig. 1A was first fit to the Hill equation (dash line in Fig. 1A) [20,21]. Next, at a particular signal (fraction of DNA retained on the NC membrane) a horizontal line is drawn which intersects each of the five isotherms. After that, the total IVa2 concentration associated with each point of intersection is determined, which is then paired with the corresponding total DNA concentration (i.e. we determine five pairs of $L_{t,i}$, $D_{t,i}$), as shown in Fig. 1A [20]. Finally, we repeated this analysis by drawing a series of horizontal lines from $Y = 0.05$ to 0.85, where Y is the fraction of signal retained on the NC membranes. The resulting groups of IVa2 and DNA concentrations are plotted against each other and fitted to straight lines (as illustrated in Fig. 1B). This analysis shows a linear relationship between the total IVa2 and DNA concentrations. The slope of each linear fit (solid lines in Fig. 1B) represents the degree of binding (i.e. the average number of IVa2 bound to a DNA molecule) and the intercept represents the concentration of free IVa2 protein for each selected fraction of signal retained on the NC

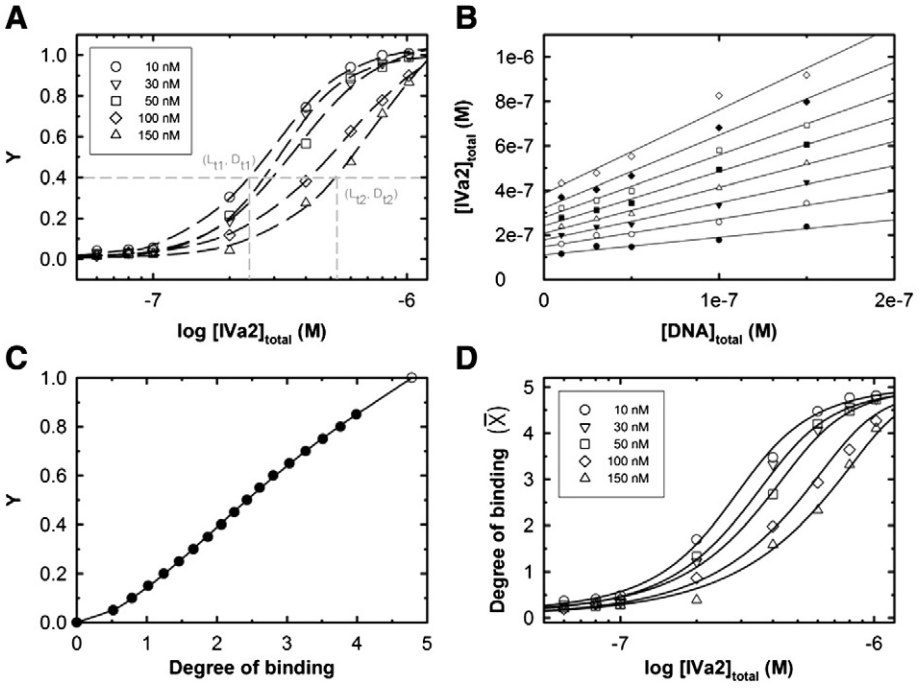

Fig. 1. *Macromolecular Binding Density Function (MBDF) analysis of the filter binding experiments investigating the binding of the IVa2 protein to the 109 bp DNA.* (A) The amount of radioactivity retained on the nitrocellulose (NC) and DE membranes was quantified and the fraction of DNA retained on the NC membrane (Y) was plotted vs the total IVa2 concentration. The dashed line corresponds to an NLLS fit of the data to the Hill Equation, to help guide the MBDF analysis. A horizontal line was drawn at a particular value of Y. Next, vertical lines were drawn at the intersections of each DNA concentration. The corresponding pairs of IVa2 and DNA concentrations are plotted in B over a range of Y values. The slopes of these lines represent the binding density at that particular Y value. (C) The fraction of signal retained on the NC membrane (Y) is plotted as a function of the degree of binding obtained from (B). After short extrapolations to the origin and $Y = 1$ (open circle), the data were fitted to a polynomial equation of order 4 to describe empirically the relationship between Y and the degree of binding (solid line). (D) The function obtained in (C) was used to convert the titrations in (A) into the degree of binding as a function of the total IVa2 concentration. The transformed data were then analyzed according to the MvH non-specific binding model (solid lines).

membranes (Y) [20]. Fig. 1C shows the degree of binding plotted as a function of the fraction of DNA retained on the NC membrane (Y). It is clear Y is not linearly proportional to the degree of binding. Thus, we have to take this non-linearity into account when modeling these data. A short extrapolation to $Y = 1$ (open circle) provides us with the stoichiometry of binding of the IVa2 protein to the DNA. From this analysis, we estimate a saturated stoichiometry of ~5 IVa2 to this 109 bp DNA. We then fit the data in Fig. 1C to a polynomial (solid line) in order to obtain a function that describes the relationship between Y and the degree of binding [21]. This function was then used to convert the fraction of DNA retained on the NC membrane into the degree of binding, and the results are shown in Fig. 1D.

Next, we performed an NLLS analysis of these data using the McGhee–von Hippel (MvH) non-specific binding model in order to resolve the intrinsic non-specific binding constant (K_{ns}), occluded site size (n) and nearest-neighbor cooperativity (w). The smooth curves shown in Fig. 1D are the results of a global, NLLS analysis of all five DNA concentrations according to Eq. (1), which returns best fit parameters of $K_{ns} = 3.1\ (2.2, 4.3) \times 10^4\ M^{-1}$, $w = 146\ (100, 213)$ and $n = 21.5$ bp (single set of experiments under 5 different concentrations of DNA, Table 1). We repeated this analysis for a longer DNA of 241 bp. The results of this analysis are shown in Fig. 2 and Table 1 and result in essentially identical estimates for K_{ns}, w and n.

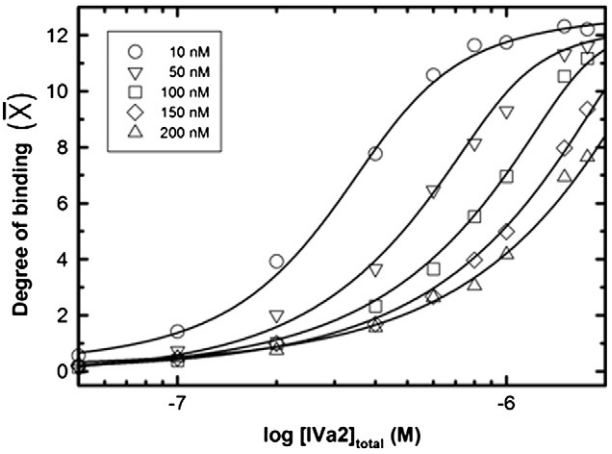

Fig. 2. *Non-specific binding of IVa2 to a 241 bp DNA.* Five different concentrations of the 241 bp DNA were titrated with IVa2 and the fraction of DNA bound was determined using the filter binding technique. The data were analyzed according to the MBDF analysis as described. The solid lines are the NLLS analysis of the data according to the MvH non-specific binding model.

4. Sedimentation equilibrium studies to determine the distribution of IVa2 on non-specific DNA

We designed a sedimentation equilibrium experiment to independently determine the distribution of IVa2 ligation states to the non-specific DNA. Sedimentation equilibrium provides direct information on the molecular weight of the protein-DNA complex, which allows direct calculation of the number of IVa2 molecules bound to the DNA molecule. These studies were carried out using a 241 bp DNA which contained a Cy3 dye at each end. To achieve enough absorbance signal for accurate detection in the XLA, we loaded 0.65 μM of the DNA into each channel. At these high DNA concentrations, the binding reactions are expected to occur under stoichiometric conditions.

Fig. 3 shows sedimentation equilibrium experiments performed at 0.65 μM of the 241 bp DNA with four different loading concentrations of the IVa2 protein: 0.50, 2.0, 3.0, and 4.3 μM, in Buffer H at 25 °C. The mixtures were sedimented to equilibrium at three rotor speeds (5.0, 7.5 and 10 K RPM), and the concentration distributions of the DNA species – i.e. the free DNA and all protein DNA bound species – were monitored by absorbance at 522 nm. The samples reached sedimentation equilibrium within 75 h for the first speed and 48 h for both the second and third speeds.

The apparent buoyant molecular weight was estimated by fitting each concentration, at each speed, to a single, ideal species model. This simple analysis has been shown to approximate the z-average buoyant molecular weight of the sample in the cell [26], and is used here only to compare approximately the degree of binding between the sedimentation equilibrium and filter binding techniques. This was accomplished by solving Eq. (7) for m, and then comparing this with the expected values from the analysis of the filter binding data (solid line in Fig. 4 was generated using the values shown in Table 1). This comparison demonstrates that at 0.65 μM 241 bp DNA, the binding reaction occurs under stoichiometric conditions. In addition we see that two fundamentally different techniques (sedimentation equilibrium and nitrocellulose filter binding) produce similar estimates for the degree of binding over a range of IVa2:DNA molar ratios (Fig. 4). However, we were unable to perform these experiments at IVa2 concentrations higher than 4.3 μM, due to sample precipitation. This experimental limitation prevents us from using this simple analysis to directly estimate the occluded site size, since we cannot increase the IVa2 concentration high enough to observe a break point. However, the shape of the sedimentation equilibrium concentration distribution is sensitive to both n and w, since both of these parameters determine the distribution of IVa2 ligation states on the DNA molecule. For example, large values of w will result in sedimentation equilibrium distributions containing many more DNA molecules with long clusters of IVa2 bound. On the other hand, as n is increased, it becomes progressively more difficult to load the next ligand onto the lattice, which tends to disfavor longer clusters. These considerations suggest that a direct, NLLS analysis of the primary concentration distributions will provide information on the cooperativity and occluded site size. To carry out this analysis, we have developed a method to analyze sedimentation equilibrium data using the MvH model.

The smooth curves in Fig. 3 are the results of this NLLS analysis (Eqs. (10)–(12)). In this analysis, we have fixed the values for K_{ns}, n and w to the values shown in Table 1, while allowing the free concentrations of IVa2 and DNA at the sample meniscus to vary in the fitting. As can be seen by the excellent agreement between the model and the experimental data, this analysis describes the experimental data very well. Next, these best fit values (i.e. concentrations) were used to extrapolate the data collected at each rotor speed, for each IVa2:DNA loading ratio, to a single, common position at the base of the cell (r_b) assuming mass conservation (using Eq. (14)). The resulting estimates for the base of the cell are shown in Table 2, and are also shown in Fig. 3 as the point where extrapolation of the smooth curves terminates. If the value of K_{ns} is unreasonable and/or the model is incorrect, the resulting estimates for the base of the cell will be physically unrealistic,

Table 1
Summary of filter binding experiments on IVa2 nonspecific binding thermodynamics.[a]

DNA	K_{ns} (M^{-1})	w [b]	n [c] (bp)
109 bp[d]	$3.1\ (2.2, 4.3) \times 10^4$	146 (100, 213)	21.5
241 bp[e]	$4.2\ (\pm 0.7) \times 10^4$	118 (±14)	17.8 (±1.4)
Average[f]	$3.9\ (\pm 0.6) \times 10^4$	125 (±12)	18.8 (±1.4)

[a] Non-specific (NS) 109 bp and 241 bp data were globally analyzed using Eqs. (1) and (2).
[b] Nearest-neighbor cooperativity.
[c] Number of nucleotides occluded in nonspecific binding.
[d] Single set of experiments with five concentrations of DNA. Experimental errors were evaluated using F-statistics at a 68.3% confidence level.
[e] The average and standard deviation of the mean from three sets of experiments, each with five concentrations of DNA.
[f] The average (±standard deviation of the mean) of four sets of experiments using 109 and 241 bp DNA

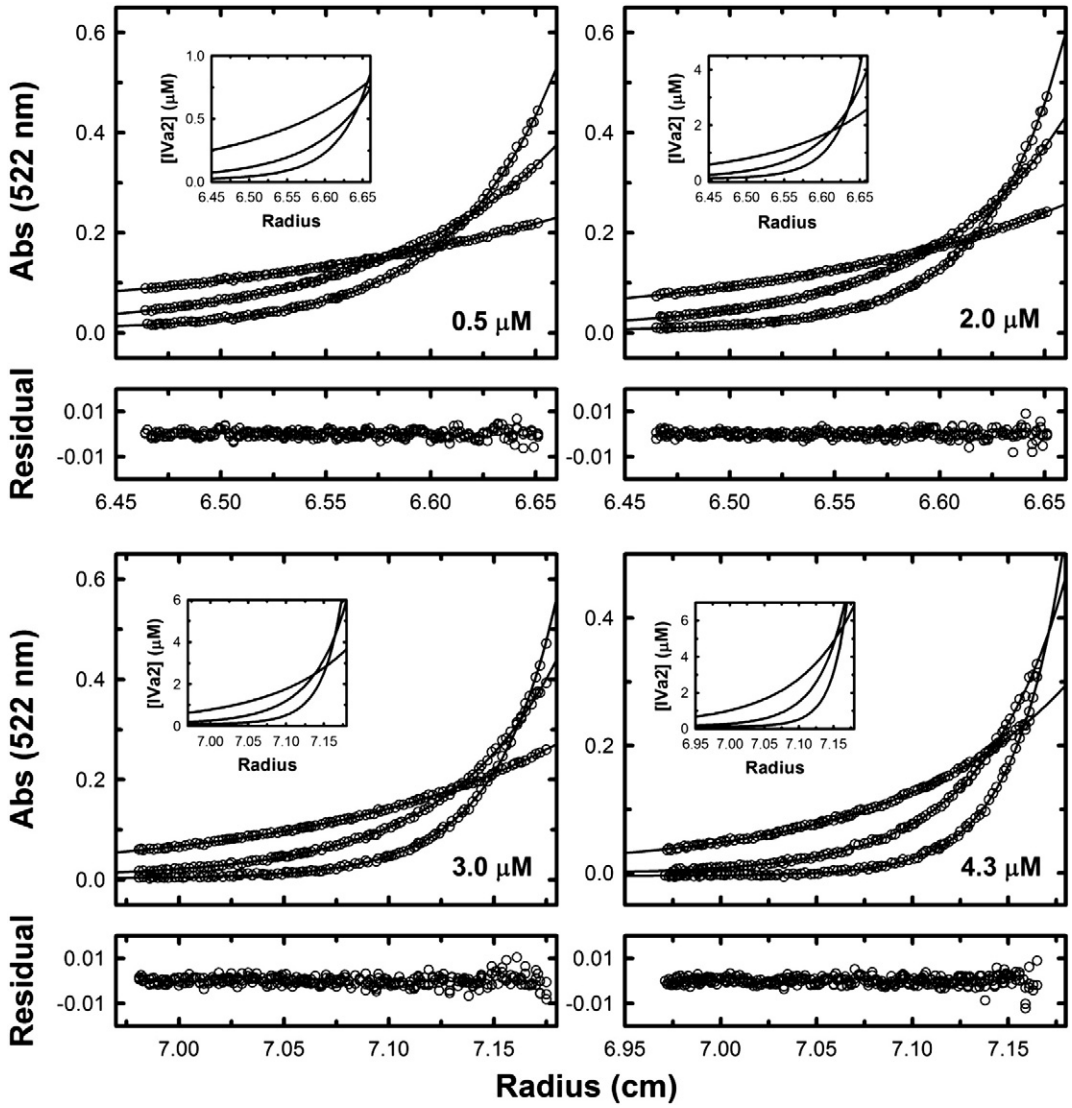

Fig. 3. *NLLS analysis of the primary sedimentation equilibrium data using the MvH model.* The data in Fig. 3 were analyzed by NLLS according to the MvH model (Eqs. (10)–(12)). The smooth curves are the results of this analysis fixing K_{ns}, w and n at the values determined from the filter binding data: $K_{ns} = 3.9 \times 10^4\ M^{-1}$, $w = 125$, and $n = 18.8$ bp (Table 1). In this analysis, the concentrations of free IVa2 protein and free 241 bp (Cy3) DNA at the meniscus position, $L_{f,m}$ and $D_{f,m}$, were allowed to float. The insets shows the predicted concentration distributions of the total IVa2 protein calculated at 5, 7.5 and 10 K RPM, using the best fit parameters from the NLLS analysis.

which is not what we observe. Table 2 shows that the estimated values at the base of the cell are in good agreement with the known values.

Next, we investigated if the shape of the sedimentation equilibrium curves could provide information on the range of possible values of n and w. To accomplish this, we carried out an iterative NLLS approach utilizing mass conservation constraints, since it is not possible to obtain an analytical solution for the total loading concentration of the ligand or the DNA by integration. This was achieved by carrying out NLLS fits over a range of values of n and w, and then calculating the predicted total IVa2 and DNA concentrations via numerical integration using Eqs. (13) and (14). The integration was carried out starting at r_m and finishing at our best estimate of r_b (Table 2). Next, the calculated loading IVa2 and DNA concentrations were compared with the known loading concentrations. The lower limit of w and the upper limit of n were well constrained since values outside these limits returned total IVa2 concentrations in excess to those loaded in the cell, which is physically impossible. On the other hand, the upper limit of w and the lower limit of n were well constrained by noting a significant decrease in the quality of the fit (68% CI from F-statistics). This analysis resulted in ranges of n and w of (13–31) and (79–175), respectively. These ranges are consistent with our filter binding results.

5. Discussion

The Ad IVa2 protein is required for at least two viral processes: late gene transcription and DNA packaging. Previous studies have shown that the viral DNA packaging reaction requires at least two additional viral components: the viral L4-22 K protein and the viral packaging sequence DNA [9–13]. In the presence of both IVa2 and L4-22 K proteins, they specifically interact with conserved DNA elements, called A repeats, in the viral packaging sequence [9–11,13–15], although they do not detectably interact with each other in the absence of specific DNA. While L4-22 K requires IVa2 to specifically load onto DNA containing A repeats, the IVa2 protein possesses strong non-specific DNA binding activity. In contrast with L4-22 K, IVa2 can also recognize the A sequence DNA by itself, albeit with only modest (~10 fold) specificity [17]).

Since IVa2 binds ds DNA with strong positive cooperativity, it is expected it will form clusters on the adenoviral genome *in vivo*. To quantify the size and distribution of these clusters, we have calculated the average cluster size, <q> (Eq. (13) from [1]) [1], as well as the probability distribution of cluster sizes p(q) (Eq. (6) from [29], Fig. 5). These calculations were performed using $w = 125$; $n = 18.8$ bp. At low fractional saturation ($f \leq 0.1$), the majority of the IVa2 is bound to the DNA in a

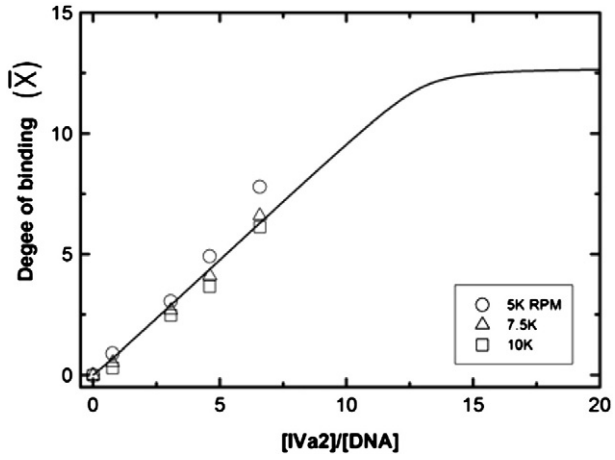

Fig. 4. *Sedimentation equilibrium analysis of the non-specific binding of IVa2 to the 241 bp DNA under stoichiometric binding conditions.* 0.65 μM 241 bp (Cy3) DNA was mixed with four different loading concentrations of IVa2 (0.5, 2.0, 3.0 and 4.3 μM) in Buffer H (25 °C). The samples were sedimented to equilibrium at 3 rotor speeds: 5.0, 7.5, and 10 K RPM, and the concentration distributions were recorded at 522 nm. An estimate of the degree of binding for each sample was obtained using Eq. (7) and plotted as a function of the ratio of the loading concentrations of IVa2 and DNA. The smooth curve is the predicted isotherm using the MvH model (Eqs. (1) and (2)), and the parameters determined from NLLS analysis of the filter binding titrations (Table 1) for 241 bp DNA.

singly ligated state. High fractional saturations ($f \geq 0.8$) are required to produce larger cluster sizes (Fig. 5B). These simulations show that formation of IVa2 clusters is limited; i.e. IVa2 does not easily saturate the dsDNA through positive cooperative interactions, in contrast to other systems, such as the phage T4 gene 32 binding protein ($w \sim 2000$) [30]. A consequence of this is that other proteins have access to the DNA, such as the Ad L4-22 K protein. One possibility is that limited IVa2 clusters play a role in recruiting L4-22 K to the DNA, after which the IVa2 and L4-22 K proteins together locate the PS for specific assembly. Other possibilities exist that have precedent in the literature, such as "tunable" cluster sizes which are modulated by salt concentration and type, pH and even binding density (e.g. *E. coli* SSB, ss DNA binding protein [31]).

Our recent experiments have shown that several L4-22 K and IVa2 stoichiometries can be assembled onto A repeats [17]. Of particular interest in these studies is the observation that the binding of a single L4-22 K monomer, presumably between two IVa2 binding sites, strongly promotes positive cooperative binding of two IVa2 monomers on either side of the L4-22 K [17]. We speculated that L4-22 K "relocates" non-specifically bound IVa2 to the A repeats by promoting positive cooperative interactions between the two IVa2 monomers. In this scenario, IVa2 does not freely diffuse in the crowded nucleus to find the specific binding sites within the PS, but rather is relocated via one-dimensional diffusion along the Ad genome until it reaches the PS. According to this hypothesis, these steps represent the first molecular events that initiate the virus assembly process.

Table 2
Estimate of the base position from sedimentation equilibrium using mass conservation approach.

[IVa2] (μM)	Estimated r_b (cm)[a]	Known r_b (cm)[b]
0.5	6.6726	6.6923
2.0	6.6756	6.6928
3.0	7.1983	7.2184
4.3	7.2013	7.2191

[a] The positions of the base of the cell were estimated using Eq. (14).
[b] The known positions of the base of the cell were determined from a sedimentation equilibrium experiment using a 48 bp ds DNA, and applying mass conservation constraints during a global, NLLS analysis of the experimental data; see Refs. [16,25].

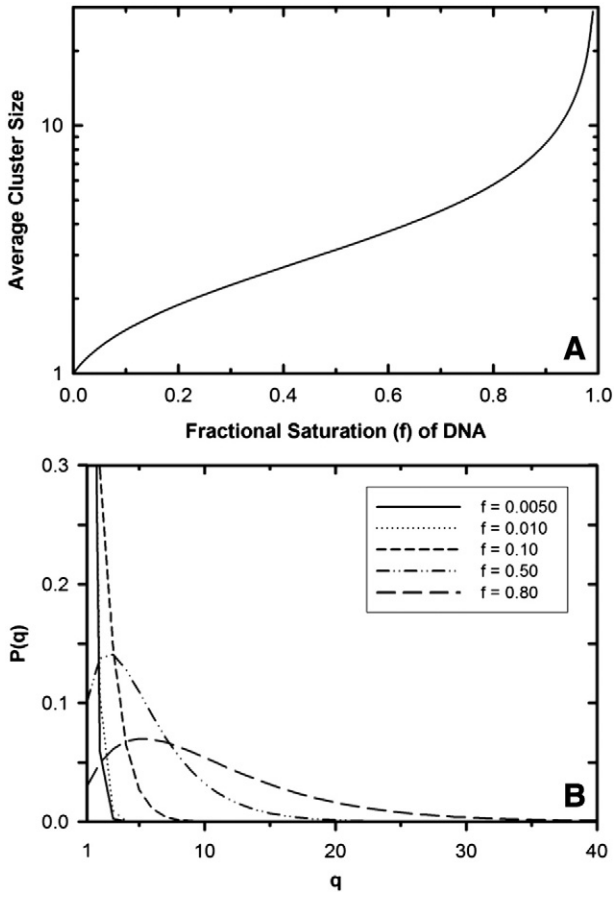

Fig. 5. The prediction of average IVa2 cluster size and the probability distribution of a particular cluster size under infinite length DNA (A) The predicted average cluster size, $<q>$, of IVa2 is plotted as a function of fractional saturation (f) of the DNA using Eq. (13) from [1] with $n = 18.8$ and $w = 125$ [1; 34]. (B) The probability distributions ($P(q)$) of a particular IVa2 cluster size, q, were calculated at the indicated values of the fractional saturation (f) of the DNA according to Eq. (6) in [27].

Acknowledgment

We thank Drs. Thomas Record, Jr. and Oleg Tsokidov for discussions concerning the derivation of Eq. (9) in the text.

References

[1] J.D. McGhee, P.H. von Hippel, Theoretical aspects of DNA–protein interactions: co-operative and non-co-operative binding of large ligands to a one-dimensional homogeneous lattice, J. Mol. Biol. 86 (1974) 469–489.
[2] M.J. McConnell, M.J. Imperiale, Biology of adenovirus and its use as a vector for gene therapy, Hum. Gene Ther. 15 (2004) 1022–1033.
[3] P. Ostapchuk, P. Hearing, Control of adenovirus packaging, J. Cell. Biochem. 96 (2005) 25–35.
[4] T. Kojaoghlanian, P. Flomenberg, M.S. Horwitz, The impact of adenovirus infection on the immunocompromised host, Rev. Med. Virol. 13 (2003) 155–171.
[5] P. Ljungman, Treatment of adenovirus infections in the immunocompromised host, Eur. J. Clin. Microbiol. Infect. Dis. 23 (2004) 583–588.
[6] P. Lutz, C. Kedinger, Properties of the adenovirus IVa2 gene product, an effector of late-phase-dependent activation of the major late promoter, J. Virol. 70 (1996) 1396–1405.
[7] G. Mondesert, C. Tribouley, C. Kedinger, Identification of a novel downstream binding protein implicated in late-phase-specific activation of the adenovirus major late promotor, Nucleic Acids Res. 20 (1992) 3881–3889.
[8] C. Tribouley, P. Lutz, A. Staub, C. Kedinger, The product of the adenovirus intermediate gene IVa2 is a transcriptional activator of the major late promoter, J. Virol. 68 (1994) 4450–4457.
[9] S.G. Ewing, S.A. Byrd, J.B. Christensen, R.E. Tyler, M.J. Imperiale, Ternary complex formation on the adenovirus packaging sequence by the IVa2 and L4 22-kilodalton proteins, J. Virol. 81 (2007) 12450–12457.
[10] M. Grable, P. Hearing, Adenovirus type 5 packaging domain is composed of a repeated element that is functionally redundant, J. Virol. 64 (1990) 2047–2056.

[11] P. Ostapchuk, M.E. Anderson, S. Chandrasekhar, P. Hearing, The L4 22-kilodalton protein plays a role in packaging of the adenovirus genome, J. Virol. 80 (2006) 6973–6981.
[12] S.I. Schmid, P. Hearing, Bipartite structure and functional independence of adenovirus type 5 packaging elements, J. Virol. 71 (1997) 3375–3384.
[13] R.E. Tyler, S.G. Ewing, M.J. Imperiale, Formation of a multiple protein complex on the adenovirus packaging sequence by the IVa2 protein, J. Virol. 81 (2007) 3447–3454.
[14] P. Ostapchuk, J. Yang, E. Auffarth, P. Hearing, Functional interaction of the adenovirus IVa2 protein with adenovirus type 5 packaging sequences, J. Virol. 79 (2005) 2831–2838.
[15] W. Zhang, M.J. Imperiale, Interaction of the adenovirus IVa2 protein with viral packaging sequences, J. Virol. 74 (2000) 2687–2693.
[16] T.C. Yang, Q. Yang, N.K. Maluf, Interaction of the adenoviral IVa2 protein with a truncated viral DNA packaging sequence, Biophys. Chem. 140 (2009) 78–90.
[17] T.C. Yang, N.K. Maluf, Cooperative heteroassembly of the adenoviral L4-22 K and IVa2 proteins onto the viral packaging sequence DNA, Biochemistry 51 (2012) 1357–1368.
[18] A. Pardo-Mateos, C.S. Young, A 40 kDa isoform of the type 5 adenovirus IVa2 protein is sufficient for virus viability, Virology 324 (2004) 151–164.
[19] I. Wong, T.M. Lohman, A double-filter method for nitrocellulose-filter binding: application to protein-nucleic acid interactions, Proc. Natl. Acad. Sci. U. S. A. 90 (1993) 5428–5432.
[20] T.M. Lohman, W. Bujalowski, Thermodynamic methods for model-independent determination of equilibrium binding isotherms for protein–DNA interactions: spectroscopic approaches to monitor binding, Methods Enzymol. 208 (1991) 258–290.
[21] W. Bujalowski, Thermodynamic and kinetic methods of analyses of protein-nucleic acid interactions. From simpler to more complex systems, Chem. Rev. 106 (2006) 556–606.
[22] W. Bujalowski, T.M. Lohman, C.F. Anderson, On the cooperative binding of large ligands to a one-dimensional homogeneous lattice: the generalized three-state lattice model, Biopolymers 28 (1989) 1637–1643.
[23] O.V. Tsodikov, J.A. Holbrook, I.A. Shkel, M.T. Record Jr., Analytic binding isotherms describing competitive interactions of a protein ligand with specific and nonspecific sites on the same DNA oligomer, Biophys. J. 81 (2001) 1960–1969.
[24] J. Wyman, S.J. Gill, Binding and linkage, University Science Books, 1990.
[25] J.W. Ucci, J.L. Cole, Global analysis of non-specific protein–nucleic interactions by sedimentation equilibrium, Biophys. Chem. 108 (2004) 127–140.
[26] T.M. Laue, Sedimentation equilibrium as thermodynamic tool, Methods Enzymol. 259 (1995) 427–452.
[27] J. Vistica, J. Dam, A. Balbo, E. Yikilmaz, R.A. Mariuzza, T.A. Rouault, P. Schuck, Sedimentation equilibrium analysis of protein interactions with global implicit mass conservation constraints and systematic noise decomposition, Anal. Biochem. 326 (2004) 234–256.
[28] D.F. Senear, M. Brenowitz, M.A. Shea, G.K. Ackers, Energetics of cooperative protein-DNA interactions: comparison between quantitative deoxyribonuclease footprint titration and filter binding, Biochemistry 25 (1986) 7344–7354.
[29] T.M. Lohman, Model for the irreversible dissociation kinetics of cooperatively bound protein-nucleic acid complexes, Biopolymers 22 (1983) 1697–1713.
[30] S.C. Kowalczykowski, N. Lonberg, J.W. Newport, P.H. von Hippel, Interactions of bacteriophage T4-coded gene 32 protein with nucleic acids. I. Characterization of the binding interactions, J. Mol. Biol. 145 (1981) 75–104.
[31] W. Bujalowski, L.B. Overman, T.M. Lohman, Binding mode transitions of *Escherichia coli* single strand binding protein-single-stranded DNA complexes. Cation, anion, pH, and binding density effects, J. Biol. Chem. 263 (1988) 4629–4640.